Surface and pore modification of tripolyphosphate-crosslinked chitosan/polyethersulfone composite nanofiltration membrane; characterization and performance evaluation

Zahra Afsarian and Yaghoub Mansourpanah[†]

Membrane Research Laboratory, Lorestan University, 68137-17133 Khorramabad, Iran
(*Received 24 November 2017 • accepted 27 May 2018*)

Abstract−A PES-based composite nanofiltration membrane was prepared by spreading a thin layer of sodium tripolyphosphate (STPP)-modified chitosan (CS) on a PES membrane. Two approaches of modification were employed: coating, and injecting the chitosan solution into PES membrane by applying pressure. Physicochemical properties of the prepared membranes were characterized by FTIR-ATR, zeta potential, contact angle, AFM and FE-SEM methods. AFM images showed a denser and more compact surface for STPP-modified membranes compared to the unmodified one. The membranes prepared by the second approach illustrated favorable properties: the increase of both flux and rejection. Engaging of -NH$_2$ groups in CS with polyanionic phosphate groups of STPP resulted in less availability of functional groups. Furthermore, denser and relatively higher positively charged surface could be the main reasons for higher rejection of membrane composed of 0.05 wt% STTP towards copper ions in comparison with the other membranes. Furthermore, the presence of SO$_4^{2-}$ ions in the CuSO$_4$ solution slightly changed the positive charge of the membrane surface, resulting in tangible variations in rejection. According to the Donnan exclusion theory, relative increase of the negative charge of the surface in the presence of the highest concentration of STTP caused less NaCl and CuSO$_4$ rejection compared to the other STPP modified membranes.

Keywords: Polyethersulfone Membrane, Thin Film Composite, Chitosan, Sodium Tripolyphosphate, Metal Ions Removal

INTRODUCTION

As a remarkable and impressive separation technology, membrane processes have gained new importance in the separation and purification of water as well as recovery and pollution control in recent years [1-3]. Nanofiltration (NF) is fairly new pressure-driven membrane separation technology that has significantly grown in the world in the past few decades [4,5]. The membrane process based on NF technology has been widely employed in industrial water production, water softening, pharmaceuticals, chemicals, paper production, and wastewater treatment as well as seawater desalination [6,7].

With rapid industrial development such as mining operations, fertilizer industries and metallurgy, a large amount of wastewater comprising heavy metals is evacuated into bodies of water [8]. Unlike some organic pollutants, heavy metals are not biodegradable, cannot be decomposed and tend to accumulate in living organisms. Heavy metal toxicity has detrimental effects on human physiology and ecological systems even at very low concentration [9]. So, choosing a suitable and efficient method for the removal of toxic heavy metals has become one of the major concerns in water treatment. Chemical precipitation, ion exchange, solvent extraction, adsorption, membrane filtration and electrochemical treatment are confident methods for the removal of heavy metal ions [10,11].

In the past decades, membrane processes, especially nanofiltration, have gained increasing attention as a promising and environmental technology for the removal of heavy metals because of several advantages such as higher water permeability without compromising rejections, energy saving, reducing operating costs, etc. [8,12].

Many composite NF membranes have been designed based on multi-layer composite structure, which consists of active thin layer and porous supporting layer and can be optimized individually according to the required performances of the thin layer or support layer [13].

Polyethersulfone (PES) membrane is widely used in ultrafiltration and nanofiltration due to its excellent chemical resistance, good thermal and mechanical properties and high glass transition temperature. Nevertheless, this kind of membrane shows a remarkable tendency to be adsorbed on the surface and pores due to the intrinsic hydrophobic characteristic of PES [14,15]. To get a hydrophilic surface by anti-fouling property, several techniques such as modification with suitable hydrophilic polymer via blending, coating and surface grafting [11,16] have been evaluated. Chitosan is a hydrophilic polymer utilized to modify hydrophobic membranes such as poly (vinylidene fluoride), poly (acrylonitrile) and polystyrene to enhance their hydrophilicity [15-19]. Chitosan, the N-deacetylated form of chitin, is a natural aminopolysaccharide which is one of the most plentiful natural polymers in the world second to cellulose. CS is not only non-toxic, odorless, antibacterial and biodegradable with low immunogenicity, but also possesses a high density of positive charge in an acid solution that can be attributed to the glucosamine groups on its backbone [20]. Because of these beneficial characteristics, chitosan has been employed in wastewater treatment, heavy metal ion adsorption from water, biomaterials, mem-

[†]To whom correspondence should be addressed.
E-mail: mansourpanah.y@lu.ac.ir, jmansourpanah@yahoo.com

brane materials, pharmaceuticals and nutraceuticals. These properties allow the formation of stable ionic complexes by multivalent aqueous soluble poly-anions under gentle physiological conditions. Chitosan is a polycationic polymer which can interact with negatively charged species with low molecular weight such as tripolyphosphate (TPP) through electrostatic forces creating ionic cross-linked networks. Sodium Tripolyphosphate (STPP) is a non-toxic polyanion, usually recognized as pentasodium tripolyphosphate or pentasodium triphosphate ($Na_5P_3O_{10}$), which is a straight chain derivative of phosphoric acid [21].

The amine ($-NH_2$) and hydroxyl ($-OH$) groups in the polymer chain of chitosan act as coordination sites for heavy metal ions. Metal ions can attach to amino groups in chitosan with chelation mechanism or electrostatic attraction [22].

Several studies have been carried out on fabrication of chitosan nanofiltration membranes with various reagents. Boributh et al. fabricated a chitosan membrane using PVDF as substrate for reducing protein fouling [15]. The results confirmed good antifouling properties. Miao et al. created a novel kind of thin film composite (TFC) membrane based on sulfated chitosan (SCS) via the coating and cross-linking with epichlorohydrin (ECH) [4]. Shenvi et al. synthesized a composite membrane having chitosan as the active layer supported on poly(1,4-phenylene ether-ether-sulfone) (PPEES) membrane and glutaraldehyde as cross-linking agent [1]. In another work, the same authors prepared nanoporous chitosan membranes by PPEES as support membrane and sodium tripolyphosphate (TPP) as cross-linking agent in different pHs. The membranes showed higher crosslinking density in acidic media [21].

In this paper, we fabricated a type of modified chitosan-coated TFC nanofiltration membrane using a PES membrane as substrate membrane. To achieve the desired performance, CS-modified membranes were cross-linked by STPP. Nonporous chitosan membranes were prepared using two different approaches: coating and chitosan solution flowing through the surface and body of PES membrane [15]. The effect of STPP as cross-linking agent on the membrane properties such as water flux, rejection, membrane fouling resistance, hydrophilicity and pore size was examined and the results were discussed. SEM, AFM, zeta potential, contact angle and FTIR measurements were carried out to characterize the membranes. The effects of NF membrane operating conditions on the removal of heavy metal (copper) from aqueous solutions were also investigated in detail. Batch adsorption experiments were performed to study thermodynamics and kinetics of the adsorption.

EXPERIMENTAL

1. Materials

Polyethersulfone (PES, 58 kg/mol) in powder form was purchased from BASF Company (Germany) and was used for the formation of PES porous supports. Polyvinylpyrrolidone (PVP, 25 kg/mol) as pore former, poly (ethylene glycol) 600 (PEG, 600 g/mol), acrylic acid (AA), acetic acid, NaOH, sodium tripolyphosphate (STPP), ethanol and N, N-dimethylformamide (DMF) from Merck were utilized. Chitosan and Congo red and Safranin dyes for the evaluation of pore size of the membrane were purchased from Sigma-Aldrich Company. NaCl and $CuSO_4$ salts with high purity (Merck)

were used for the assessment of ion rejections. Distilled water was used throughout the study. The chemical structure of PES, CS and STPP is depicted in Fig. S1.

2. Membrane Preparation

2-1. Preparation of PES Support

PES ultrafiltration membranes were prepared with phase inversion process through immersion precipitation technique. The casting solution for polyethersulfone support was prepared by dissolving 15 wt% PES in dimethylformamide (DMF) as solvent containing 5 wt% polyvinylpyrrolidone (PVP), 5 wt% polyethylene glycol (PEG 600) and 3 wt% acrylic acid (AA) by stirring for 4 h at 50 °C. Stirring was at 300 rpm. After the formation of a homogeneous solution, the dope solution was held at ambient temperature for 24 h to remove all remaining air bubbles. Then, the dope solution was cast on a non-woven polyester (with 80 μm thickness) using a film applicator at ambient temperature without evaporation. After coating, the support was immersed into a distilled water bath for around 24 h for removing most of the solvent and water-soluble polymer.

2-2. Fabrication of PES/CS Composite NF Membranes

To investigate the effect of different conditions on the properties of thin layers, we prepared two types of membranes as follows:

• Approach 1: Coating method. The PES support was clamped between two Teflon frames that were 0.7 cm high with 7.5×20 cm^2 inner cavity. The membranes were prepared by dissolving chitosan at different concentrations of 0.5 and 1.5 wt% in 2 wt% aqueous acetic acid solution at room temperature. The temperature was increased to 60 °C to ensure the chitosan was dissolved. Then, the obtained solution was poured on the top of PES support membrane and allowed to wet for 60 min at room temperature. The surface was rolled with a soft roller to remove any small bubbles produced during the wetting procedure. The process for the preparation of TFC membrane using CS and STPP is given by Fig. S2.

• Approach 2: The chitosan solution flowing through the surface and pores of PES substrate. Chitosan solution was injected into the support membrane under the pressure of 0.2 MPa. The preparation method consisted of two stages, each with equal time. The conditions were then changed to surface flow mode in which chitosan solution flowed without applying any pressure.

Different concentrations of CS solutions (0.5 and 1.5 wt%) were chosen to fabricate the membranes. Between these two concentrations, 1.5 wt% of CS was preferred because of showing better performance in comparison with lower concentration (more detail is discussed in section 3.1). The membranes prepared with approaches 1 and 2 were dried in an oven at 70 °C for 45 min. Then, the dried membranes were neutralized by NaOH solution (0.1 M in 50 v% water-ethanol mixture) for 30 min to ensure all chitosan acetate was converted to chitosan. Then, the membranes were cleaned by 50 v% ethanol solution for 10 min to remove the remaining NaOH and repel the osmotic crack and were then washed with DI water for 30 min eventually. Finally, the membranes were dried at 25 °C. For cross-linking, the prepared chitosan solutions were mixed with 0.05, 0.1, 0.2 and 0.5 wt% STPP. Table 1 represents the composition of obtained thin layer membranes ("M" refers to the membranes prepared in approach 1 and "T" refers to the membranes in another one).

Table 1. Composition of the prepared membranes in two categories

Name (two categories)	Concentration of CS (wt%)	Concentration of STPP (wt%)
M_0, T_0 (UF membrane)	-	-
$M_{0.5}$, $T_{0.5}$	0.5	-
$M_{1.5}$, $T_{1.5}$	1.5	-
$M_{1.5-0.05}$, $T_{1.5-0.05}$	1.5	0.05
$M_{1.5-0.1}$, $T_{1.5-0.1}$	1.5	0.1
$M_{1.5-0.2}$, $T_{1.5-0.2}$	1.5	0.2
$M_{1.5-0.5}$, $T_{1.5-0.5}$	1.5	0.5

3. Characterization of Membranes

3-1. ATR-FTIR

Chemical alterations of the thin film membranes were examined using an Equinox 55 Bruker FT-IR spectrometer from Germany with an attenuated total reflection (ATR) attachment. Totally, 32 scans were measured during IR study for each sample. The resolution of the apparatus was $4\,cm^{-1}$.

3-2. Scanning Electron Microscopy-energy Dispersive X-ray Spectroscopy (SEM-EDX)

FE-SEM apparatus was employed to obtain images of the membrane surfaces and cross sections. Membrane samples were frozen in liquid nitrogen and fractured. After being sputtered with gold they were observed by a field emission scanning electron microscope (FESEM-MIRA3, TESCAN) coupled with an energy dispersive X-ray spectroscopy (EDX).

3-3. Atomic Force Microscopy (AFM)

Atomic force microscopy (AFM, non-contact mode) was utilized to analyze surface morphology, smoothness and roughness of the membranes. AFM apparatus was Dual Scope^{TM} scanning probe-optical microscope (DME model C-21, Denmark). Small pieces of the prepared membranes ($1\,cm^2$) were cut and glued on a glass substrate. Membrane surfaces were analyzed in a scan size of $1\,\mu m \times 1\,\mu m$. Surface pore (valley) size of the membranes and roughness parameters were measured by SPM-DME software.

3-4. Hydrophilicity Evaluation of the Nanocomposite Membranes

Contact angle determines the hydrophilicity of the membrane and therefore its performance. Contact angle was measured with sessile drop method using Dynamic contact angle analyzer (G10, KRUSS, Germany). To minimize experimental error, contact angles were measured at five random locations and the mean values were reported.

3-5. Swelling

To study the swelling degree of the membrane, the membrane samples were kept in distilled water for one day at room temperature and then dried in an oven at $70\,^{\circ}C$ for 30 min. Swelling ratios (SR) of the membranes were determined by the following equation [23]:

$$SR(\%) = w_s - w_d / w_d \times 100 \tag{1}$$

where w_s and w_d are the weights of wet and oven-dried membranes, respectively. All tests were repeated three times and their average value was reported.

3-6. Surface Zeta Potential Measurement

The charge properties of NF membrane surfaces were specified by zeta potentials, which were measured with streaming current method on an electrokinetic analyzer (EKA 1.00, Anton-Paar, Switzerland). Each sample was $2\,cm \times 2\,cm$ and the chosen smooth membranes were immobilized to an adjustable slit cell. KCl solution (1.0 mmol/l) with poly (methyl methacrylate) (PMMA) as reference plate (about $50\,mm \times 38\,mm \times 10\,mm$ in size) was used for the characterization of the zeta potential of the membranes. The zeta potential was measured four times and the mean value was calculated [24].

4. Filtration Performance

An aluminum batch stirred cell of 90 mL volume capacity and maximum operating pressure of 3.0 MPa with an effective area of $12.56\,cm^2$ was utilized for filtration tests. Several membranes were prepared and loaded in the filtration cell. Filtration continued at room temperature for 1 h to obtain a constant flux. The cell was equipped with a nitrogen gas inlet to impound the liquid in the cup under fixed operating pressure of 0.6 MPa. The filtration cell was filled with 80 mL feed solution with using different ion solutions (1,000 mg/L NaCl and 200 mg/L $CuSO_4$). The permeated water was accumulated, weighted in 10 min intervals and analyzed for the determination of various ions concentration. Water flux (J) and rejection (R) were calculated using following equations:

$$J = \frac{m}{A\Delta t} \tag{2}$$

$$R\% = \left[1 - \frac{\lambda_p}{\lambda_f}\right] \times 100 \tag{3}$$

where m is the weight of permeated water, A (m^2) is membrane area, Δt is permeation time, λ_f and λ_p are ion conductivity in permeate and feed, respectively. Ion rejections were assessed by measuring feed and permeate conductivities using a conductivity meter (Hanna 8733 model, Italy) [25].

5. Determination of Molecular Weight Cut Off (MWCO)

MWCO is a characteristic of membrane pore size. Membrane performance is determined with its MWCO, which is usually described as the smallest molecular weight types for which the membrane has more than 90% rejection [4]. MWCO experiments were performed using 500 mg/L aqueous solutions of organic dyes such as Congo red (MW=696.7 g/mol) and Safranin (MW=350.84 g/mol) at $25\,^{\circ}C$ and 0.6 MPa. The concentrations of the dyes in feed and permeate samples for the rejection to be achieved were determined by UV-Vis spectrometry (Shimadzu, Japan). Absorption data were measured in maximum absorption wavelengths of 341.5 and 276.5 nm for Congo red and Safranin, respectively.

5-1. Sorption of Copper Ions on CS/STPP Membrane

Chitosan has stronger capability to adsorb Cu^{2+} from $CuSO_4$ compared to other salts [22]. Static adsorption experiments were conducted to evaluate the effect of STPP on major functional groups, which may have significant effects on the physicochemical properties of polymer chains. Copper ions were exploited under various operating conditions, namely temperatures 298, 308, 318 K and initial Cu^{2+} ion concentrations of 20, 40, 80 and 160 mg/L. Accordingly, copper solutions were prepared by dissolving hydrated copper sulfate ($CuSO_4 \cdot 5H_2O$) in water. Batch adsorption experiments were performed by drenching $2\,cm \times 2\,cm$ (wet base) pieces of chi-

tosan membranes in 50 mL copper solution for 24 h at a stirring speed of 150 rpm and various temperatures, followed by the measurement of copper concentration in the solution using a flame atomic absorption spectrophotometer. The amount of adsorbate in solid phase (q (mg/g)) was calculated by following equation:

$$q = (C_o - C_{eq}) \times V/m \qquad (4)$$

where C_o and C_{eq} are initial and equilibrium concentrations of metal ion in the liquid phase (mg/L), respectively, V is the volume of solution (L) and m is the mass of chitosan membrane (gr) [22].

RESULTS AND DISCUSSION

1. Crosslinking Reagent and Chitosan

STPP as the ionic cross-linking reagent was exploited to change and improve the properties of chitosan-modified membranes. According to Mi et al., chitosan-STPP complexes are formed through ionic interaction between charged -P-O$^-$ segments of the phosphate group and protonated NH_3^+ moieties of the chitosan molecule [26]. There are $-NH_3^+$ sites when chitosan (as a crystalline biopolymer) is dissolved in acid media. Sodium tripolyphosphate is dissolved in water to produce both hydroxyl and phosphoric ions. Based on the literature, STPP-cross-linked chitosan shows low crystallinity [26]. The mechanism of cross-linking of chitosan by STPP is assumed either ionic interaction or deprotonation. The mechanism of cross-linking of chitosan with tripolyphosphate is shown in Fig. S3.

2. Membranes in the First Category

2-1. The Effect of Chitosan Solution Concentration on the Membrane Performance

A series of NF membranes were prepared in the presence of different concentrations of CS solutions (0.5 and 1.5 wt%) using the approaches mentioned previously. As shown in Table 2, M_0 presented a pure water flux around 36 L/m^2 h. Increasing chitosan concentration caused further decrease of flux wherein $M_{0.5}$ and $M_{1.5}$ the flux values were obtained about 4.25 and 3.69 L/m^2 h, respectively. On the other hand, the rejection capability of the membranes towards NaCl and CuSO$_4$ was obviously increased. Similarly, NaCl rejection was increased from 18.79% (M_0) to 38.4% ($M_{0.5}$) and 47.09% ($M_{1.5}$). Also, the values of CuSO$_4$ rejection were increased from 32.25% (M_0) to 42.3% ($M_{0.5}$) and 70.0% ($M_{1.5}$). The reason for the alterations in flux and rejection could be described as follows.

The number of amino and hydroxyl groups was increased by increasing CS concentration. Amino groups would in turn offer more cross-linking sites enhancing the cross-linking density [13, 16]. Additionally, a dense and encompassing active layer of CS on the surface could be fabricated by increasing chitosan concentration, causing significant changes in flux and rejection. Furthermore, $M_{0.5}$ and $M_{1.5}$ showed more rejection of CuSO$_4$ in comparison with NaCl, which was consistent with size exclusion mechanism and interaction of functional groups of CS (-OH and -NH$_2$) with copper ions. For charged membranes, mobility of the ions across the membrane and Donnan exclusion are two major factors impacting on the retention rate of TFC membranes. The mobility of ions through the membrane plays an important role in the rejection rate of ions; the effective size and diffusion coefficient of ions determine their mobility. Ionic and hydration radii of different ions are depicted in Table S1. SO$_4^{2-}$ ion has largest hydration radius compared to other ones, resulting in lower mobility and diffusion. Generally, the rejection of SO$_4^{2-}$ ions is higher than that of Cl$^-$ [27]. On the other hand, Cu is an intermediate element. Despite the small size of copper ions (0.096 nm) the relatively positive charge of the surface (due to the presence of some functional groups of CS (-NH$_2$)) leads to more repulsion of higher positively charged ion, which causes much more rejection of CuSO$_4$ [28]. Accordingly, the concentration of 1.5 wt% CS was chosen as a desired concentration for preparation of the developed NF membranes. Furthermore, the rejection behavior of the membranes was obviously changed by introducing of STPP, which will be described in the following sections.

2-2. Effect of Cross-linking Reagent Concentration on the Performance of Membranes

After choosing the concentration of 1.5 wt% CS as the base concentration, the NF membranes were prepared with different concentrations of sodium tripolyphosphate (0.05, 0.1, 0.2 and 0.5 wt%) as cross-linking agent. The effect of STPP concentration on the flux and NaCl rejection of the composite membranes is shown in Fig. 1. Accordingly, there was an obvious fluctuation in flux and rejection. The NaCl rejection of $M_{1.5}$ was about 47%, which increased sharply to 94.33% for $M_{1.5-0.2}$ by increasing STPP loading. On contrary, the permeation flux of the CS-modified membranes
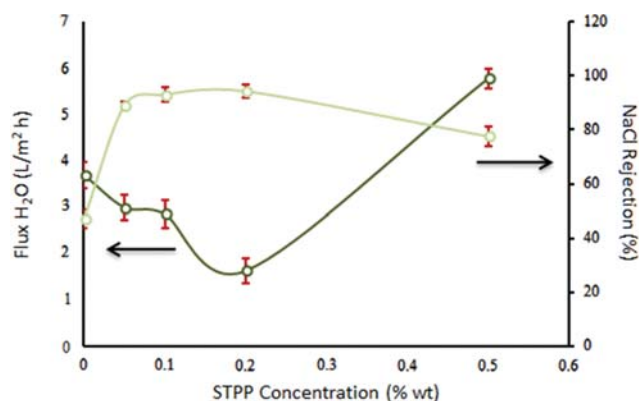
Table 2. Effect of CS concentration on the performance of membranes

Membrane	J_{wi} (L/m^2 h)	NaCl rejection (%)	CuSO$_4$ rejection (%)
M_0	36.73	18.79	32.25
$M_{0.5}$	4.25	38.4	42.3
$M_{1.5}$	3.69	47.09	70.0
$M_{1.5-0.05}$	2.99	89.04	81.0
$M_{1.5-0.1}$	2.85	93.13	56.66
$M_{1.5-0.2}$	1.63	94.33	48.33
$M_{1.5-0.5}$	5.78	77.6	43.47

Fig. 1. Effect of STPP concentration on the flux and NaCl rejection of the membranes.

decreased from 3.69 L/m^2 h ($M_{1.5}$) to 1.63 L/m^2 h ($M_{1.5-0.2}$). More loading of STPP (0.5 wt%) slightly increased flux (5.78 L/m^2 h) and decreased NaCl rejection to about 77.6%. It can be deduced that by increasing STPP concentration, the ionic interaction of chitosan and STPP led to a compact closed network structure and had increased pore tortuosity and reduced the mean size of surface holes, causing further decrease in the permeate flux and increase in the rejection [21]. However, due to some characteristics

of STPP, such as the presence of negatively charged moieties, adsorption of copper ions on the surface would relatively be increased (because of slight mitigation of positively charged surface and less availability of -NH$_2$ groups; see Fig. 3 and Table S2), resulting in relatively more diffusion and less rejection of CuSO$_4$ solution. The comprehensive reason for higher rejection of NaCl in comparison with CuSO$_4$ is described later using zeta potential data. The alterations in flux and rejection of the membrane at the highest con-
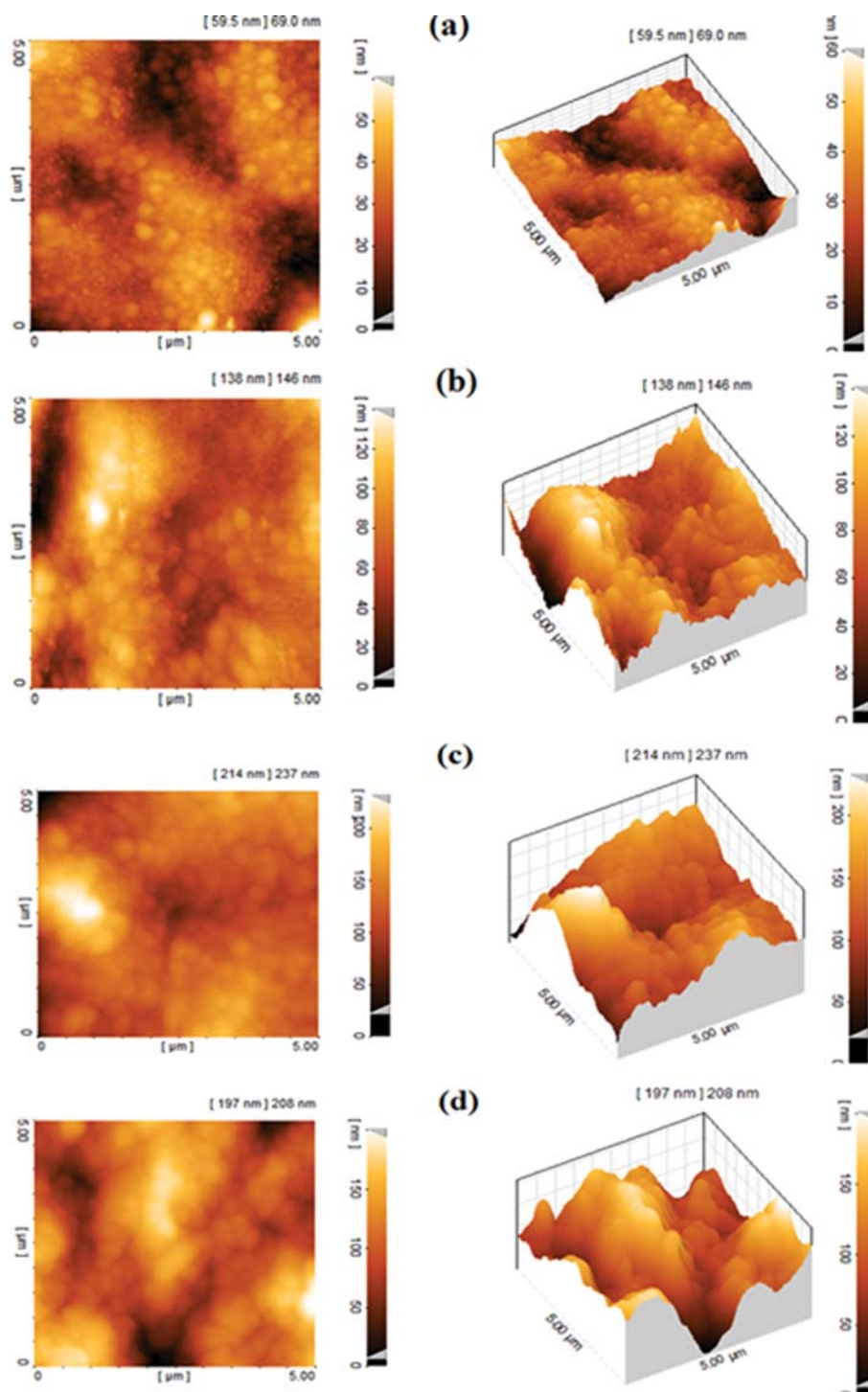

Fig. 2. AFM topographic images of: (a) $M_{1.5}$, (b) $M_{1.5-0.05}$, (c) $M_{1.5-0.2}$ and (d) $M_{1.5-0.5}$.

Table 3. The mean size of surface holes and roughness parameters of membranes (the first category)

Membrane	S_a (nm)	S_q (nm)	S_z (nm)
$M_{1.5}$	8.03	9.65	45.2
$M_{1.5-0.05}$	18.1	22.3	96.3
$M_{1.5-0.2}$	22.2	30.3	118.0
$M_{1.5-0.5}$	24.5	32.2	125.0

centration of STPP (0.5 wt%) would be described by the increase of hydrophilicity compared to the other STPP-modified membranes and more porosity of the membranes as well as changes in surface charge.

Fig. 2 shows typical 2-D and 3-D AFM images of the prepared composite NF membranes at 5 μm scale size. Accordingly, the brightest regions indicate the highest points and the dark regions present the valleys (holes) on the membrane surface. The roughness of the membranes, which are recognized in terms of mean roughness (S_a), the root mean square of Z data (S_q) and the mean difference between the highest peaks and lowest valleys (S_z), were measured by SPM DME software and are depicted in Table 3 [27].

$M_{1.5}$ (thin layer without STPP) showed a rather even surface with high porosity (Fig. 2(a)). As can be seen, there are many small and tiny spherical nodular structures on the surface of $M_{1.5}$. By increasing STPP loading by 0.2 wt%, surface properties were changed to form a dense and rough thin layer, and porosity of surface of the thin layers was decreased (Fig. 2(b), (c)). Accordingly, by higher loadings of STPP, the values of S_a, S_q, and S_z for $M_{1.5}$ were obtained to be 8.03, 9.65, and 45.2 nm, which increased to 22.2, 30.3, and 118.0 nm for $M_{1.5-0.2}$, respectively. However, the values of S_a, S_q, and S_z for $M_{1.5-0.5}$ were measured to be about 24.5, 32.2, and 125.0 nm, respectively. Creation of relatively further roughness made $M_{1.5-0.5}$ entirely different from other membranes (Fig. 2(d)), which led to higher pure water flux (5.78 L/m² h) compared to other CS-modified membranes.

Water uptake characteristic and water contact angle were evaluated to study the hydrophilic properties of the membranes. The swelling behavior of different membranes is shown in Fig. S4. As can be seen, the swelling percentages of $M_{0.5}$ and $M_{1.5}$ were about 65 and 180%, respectively. By increasing STPP loading, the swelling degree of the cross-linked membranes sharply decreased to 130% ($M_{1.5-0.05}$), 123 ($M_{1.5-0.1}$), 80% ($M_{1.5-0.2}$), and 60% ($M_{1.5-0.5}$), respectively. The higher degree of the swelling of $M_{1.5}$ compared to STPP-modified membranes could be due to the hydrophilic nature of CS. For more investigation, the water contact angles of the membranes were obtained and are given in Fig. S5. The water contact angle of M_0 was measured to be about 70° which was decreased to about 65° for $M_{1.5}$. STPP-modified membranes, however, showed higher hydrophobicity compared to unmodified membranes. Although the hydrophilicity of $M_{1.5-0.5}$ membrane (80°) was higher than that of $M_{1.5-0.05}$ (90°) and $M_{1.5-0.02}$ (100°), the hydrophilicity of $M_{1.5-0.5}$ was still lower than unmodified membrane. The reason would be that in the presence of STPP, hydrophilic (-NH₂ and -OH) groups were involved and captured during the cross-linking process (see Fig. S2), resulting in a relatively obvious decrease in the hydrophilicity of the membranes [3]. In addition, the
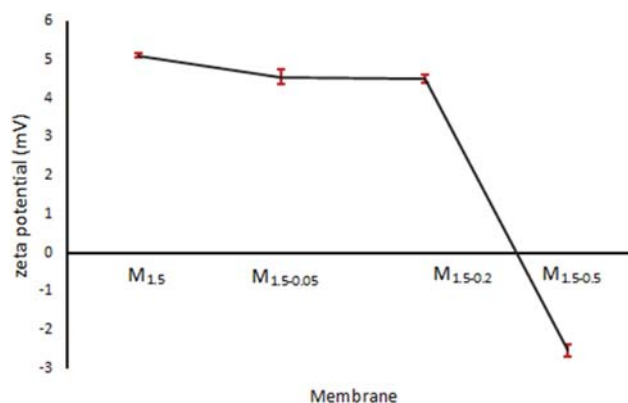
Fig. 3. Measured zeta potential of the obtained membranes.

repulsion between the functional groups of STPP molecules at the highest concentration of STPP ($M_{1.5-0.5}$) probably created further space among chains, resulting in more touching and availability of hydrophilic functional groups on the surface which slightly increased the flux.

The different rejection of the membranes towards NaCl and CuSO₄ could be explained by zeta potential data. The CS layer contains both anionic and cationic groups, while the effect of the presence of nucleophilic amino groups is stronger than hydroxyl groups, leading to the formation of positively charged membranes. According to Fig. 3, the zeta potential of $M_{1.5}$ was about +5.2 mV, which decreased linearly and slightly to +4.8 and +4.5 mV for $M_{1.5-0.05}$ and $M_{1.5-0.02}$, respectively. Furthermore, $M_{1.5-0.5}$ showed negative surface charge of about −2.5 mV. Although $M_{1.5}$, $M_{1.5-0.05}$ and $M_{1.5-0.02}$ showed positive charge on the surface, $M_{1.5-0.05}$ and $M_{1.5-0.02}$ illustrated the highest rejection towards NaCl due to the formation of a dense and compact surface on STPP-modified membranes (see Fig. 1 and descriptions). As remarked earlier, due to the presence of STPP and its effect on the charge and availability of -NH₂ groups, adsorption of copper ions on the surface would relatively be increased (Table S2), resulting in relatively more diffusion and less rejection of CuSO₄ solution (regarding the same radius of Na⁺ and Cu²⁺ ions). Less availability of protonated -NH₃⁺ in the structure of CS layer due to the interaction of protonated -NH₃⁺ in CS with polyanionic phosphate groups of STPP resulted in relative reduction of positive charges of membrane surface [26, 29]. On the other hand, due to the low solubility of STPP in water and reaching oversaturation, probably many unreacted P-O⁻ groups in STPP remained on the surface, resulting in sharp decrease of the number positive charges and creation of a slightly negatively charge membrane (about −2.5 mV).

The rejection capability of the membranes towards copper ions could also be explained. Among cross-linked membranes, $M_{1.5-0.05}$ showed the highest rejection of copper ions (81.0%). The lowest rejection towards copper ions was obtained for $M_{1.5-0.5}$ at about 43.47%. Furthermore, $M_{1.5-0.1}$ and $M_{1.5-0.2}$ illustrated rejections nearly 56.66 and 48.33%, respectively. As can be seen in Table 2, just in the case of the presence of 0.05 wt% STPP the cross-linked membrane showed favorable rejection compared to uncross-linked $M_{1.5}$ and other cross-linked ones. As stated previously, engaging of -NH₂

groups in CS with polyanionic phosphate groups of STPP resulted in less availability of functional groups for copper ions. Furthermore, the highest value of rejection for $M_{1.5-0.05}$ could be explained by its higher value of zeta potential compared to other cross-linked membranes. Although $M_{1.5-0.05}$ presented a little lower zeta potential than $M_{1.5}$, cross-linking of CS chains by STPP to form a denser surface along with a relatively high positively charged surface could be the main reason for higher rejection of $M_{1.5-0.05}$ towards copper ions compared to $M_{1.5}$. We supposed that in $M_{1.5-0.05}$ a favorable

tradeoff between the presence of functional groups of CS and STPP polyanion may create a polymeric structure with high rejection towards $CuSO_4$. As shown in Table S2, the adsorption of copper ions on the surface of the membranes was increased by increasing STPP concentration due to the interaction of functional groups of STPP with copper ions (see Fig. S6). In fact, oxygen and nitrogen atoms provided sufficient sites to interact with copper ions, leading to the passage of more copper ions through the membrane.
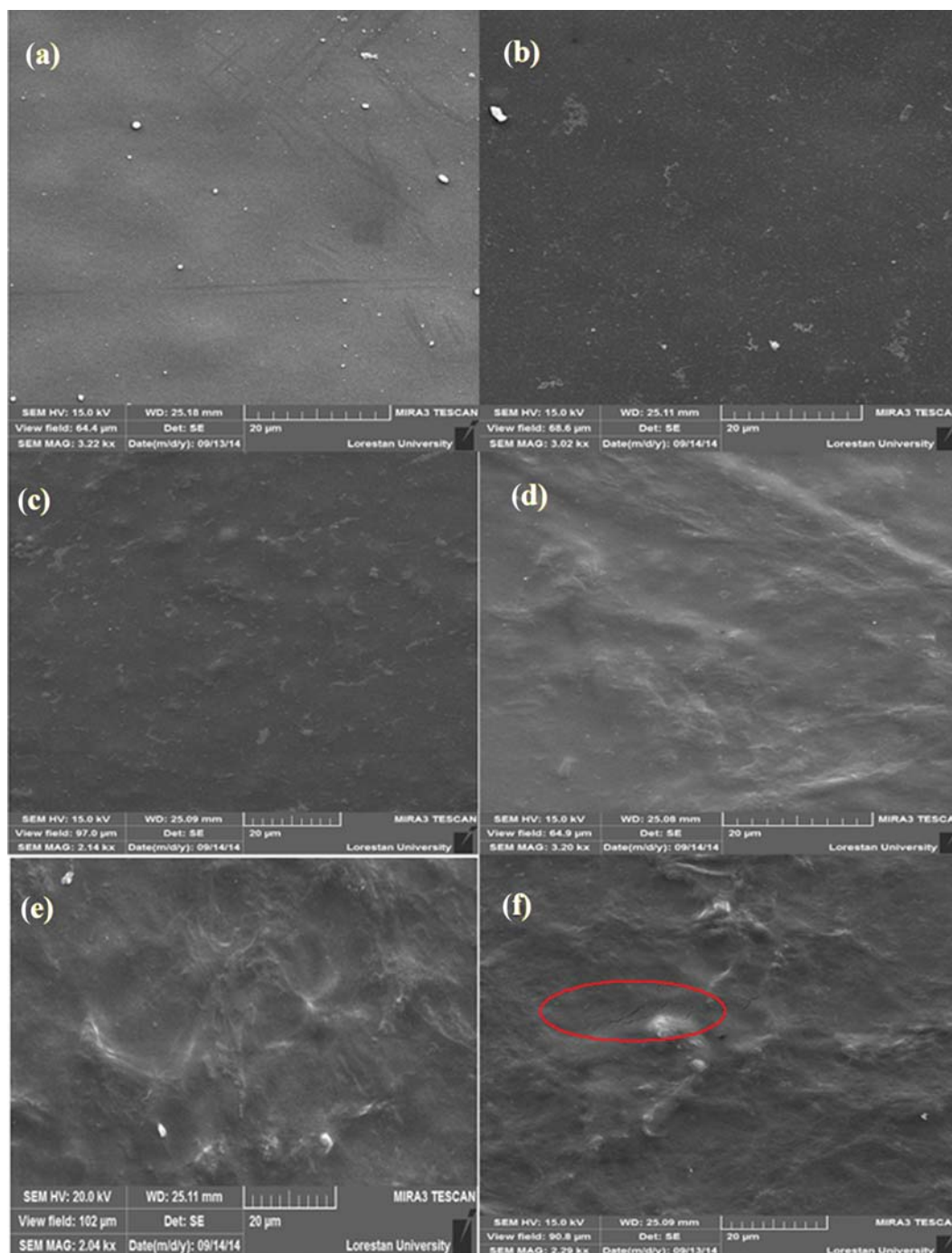

Fig. 4. Surface morphology of the composite membranes: (a) M_0, (b) $M_{1.5}$, (c) $M_{1.5-0.05}$, (d) $M_{1.5-0.1}$, (e) $M_{1.5-0.2}$ and (f) $M_{1.5-0.5}$.
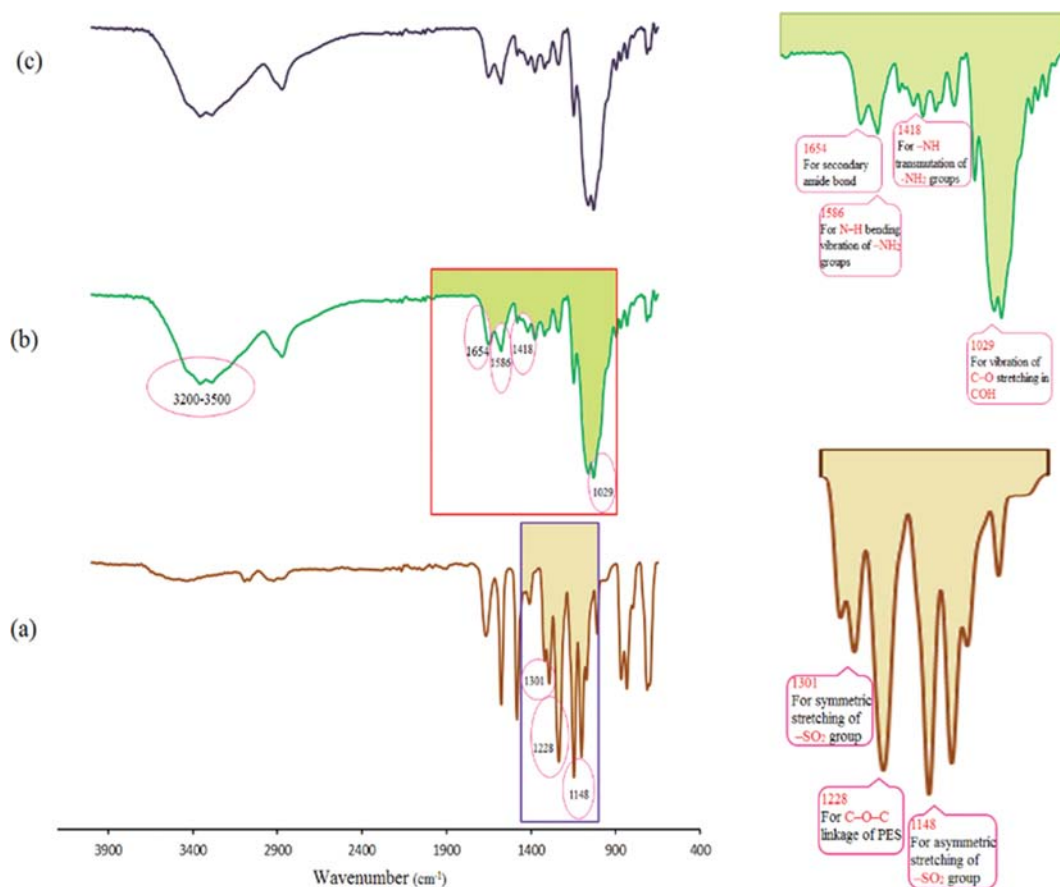
Fig. 5. ATR-IR spectra of: (a) M_0, (b) $M_{1.5}$ and (c) $M_{1.5-0.2}$.

2-3. Surface and Cross-sectional Morphology of Composite Membranes

FE-SEM images were employed to analyze the surface morphology and cross section of the membranes. Fig. 4 displays the SEM images and their corresponding EDX spectra of PES, CS and cross-linked membranes. Neat PES illustrated an even and smooth surface (Fig. 4(a)). On the other hand, CS coated-membrane showed a different surface morphology in comparison with pristine PES membrane, which proved that CS had entirely been spread on the surface (Fig. 4(b)). As can be seen, all STTP-modified membranes showed different morphologies, including uneven and rough surfaces compared to the other ones due to the effect of cross-linked structure. By increasing STPP, the surface roughness of membranes gradually increased (Fig. 4(c)-(f)). Fig. 4(f) ($M_{1.5-0.5}$) clearly shows a number of cracks on the surface of $M_{1.5-0.5}$ membrane, which is presumably the reason for lower rejection and higher flux compared to other STPP-modified membranes. As stated previously, the repulsion between functional groups of STTP molecules at the highest STTP concentration ($M_{1.5-0.5}$) probably caused further space among chains, which led to the appearance of cracks in the structure of CS layer (comprehensive explanation has been given previously).

The cross sectional SEM images of neat membrane and CS-modified membrane ($M_{1.5}$) are illustrated in Fig. S7. As shown in Fig. S7(b) ($M_{1.5}$), the thickness of the barrier layer on the surface, which is responsible of separation performance of the membranes, is much higher than that of PES membrane (Fig. S7(a), M_0). Consequently, decrease of flux and increase of rejection could be anticipated. The changes observed in flux and rejection ability of the membranes were described previously.

2-4. FTIR-ATR Analysis

FTIR-ATR analysis was exploited to characterize different functional groups presented on the surface of membranes. FTIR-ATR spectrum obtained for the neat PES membrane is shown in Fig. 5(a). The spectral bands at 1,301 and 1,148 cm^{-1} corresponded to symmetric and asymmetric stretching of -SO_2 group, respectively. The band obtained at 1,228 cm^{-1} was attributed to C-O-C bond [3]. Fig. 5(b) represents the IR spectrum of PES/CS composite film. The spectrum shows characteristic chitosan peaks at 1,029, 1,418, 1,586, 1,654, 3,500 cm^{-1}, which were thought to be due to the skeletal vibration of C-O stretching in COH, -NH transmutation vibration of -NH_2 groups, -N-H bending vibration of -NH_2 groups, the secondary amide bond of the remaining acetamido groups and O-H stretch vibration, respectively [30,31]. In the presence of STPP the band of -NH_2 was slightly widened and the small changes could be attributed to low values of STPP (Fig. 5(c), $M_{1.5-0.05}$) [26].

2-5. Molecular Weight Cut-off

Pore morphology, i.e., the average pore size and pore size distribution, plays an important role in the performance of nanofiltration membranes. Among different methods, molecular weight cut-
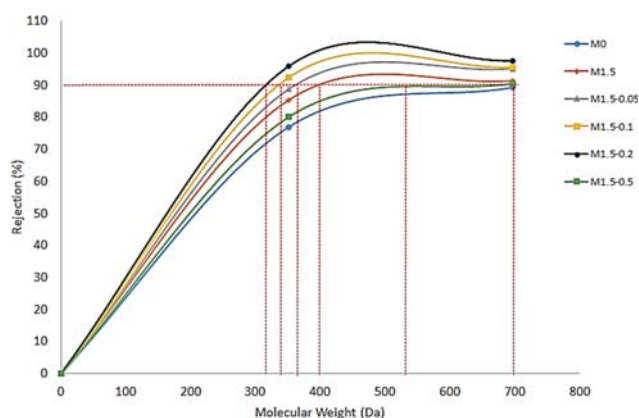
Fig. 6. MWCO curves of the composite membranes (the first category).

off technique is a favorable approach to determine the pore size of membranes [32]. The value of MWCO is shown in Fig. 6. It can be seen that the rejections of two selected dyes were higher than that of the unmodified membrane. Based on Fig. 6, the MWCO of the PES membrane was over 700 Da. In the modified membranes the value of rejection was first increased for 0.2 wt% STPP loading and was then decreased for the modified membrane with the highest amount of STPP ($M_{1.5-0.5}$). $M_{1.5}$ shows MWCO of about 400 Da. On the other hand, the membranes modified with 0.05, 0.1 and 0.2 wt% STPP presented MWCOs of 370, 335 and 310 Da, respectively. Accordingly, this suggested that for STPP-modified membranes containing 0.2 wt% STPP, a denser and more compressed CS structure along with positively charged surface would be fabricated, resulting in an obvious reduction of the size of membrane pores and increase of rejection. As stated, the repulsion of functional groups of STTP molecules in $M_{1.5-0.5}$ probably created further space among chains, resulting in the increase of MWCO. As illustrated in Fig. 6, the MWCO of $M_{1.5-0.5}$ was obtained to be about 700 Da, which was higher than other STPP-modified membranes.

3. The Second Category of Membranes

3-1. Flux and Rejection Properties of NF Membranes

The effect of CS and STPP concentrations on the performance of the second category was investigated and the results are depicted in Table S3 and Fig. S8. Accordingly, by increasing CS concentration, the pure water flux was decreased. On the other hand, much higher flux reduction was observed for STPP-modified membranes. Similarly, the flux of T_0 (neat PES membrane) was about 36.73 L/m² h, which decreased sharply to 9.48 and 9.25 L/m² h for $T_{0.5}$ and $T_{1.5}$, respectively. In addition, the flux of $T_{1.5-0.05}$, $T_{1.5-0.1}$ and $T_{1.5-0.2}$ decreased to 6.58, 5.88, and 5.61 L/m² h, respectively. Furthermore, the flux of $T_{1.5-0.5}$ slightly increased to 7.5 L/m² h. However, with loading of STPP concentration at 0.2%, the rejection ability of the membranes towards NaCl increased from 18.79% (T_0) to 96.74% ($T_{1.5-0.2}$). On the other hand, the NaCl rejection of $T_{1.5-0.5}$ decreased to 79.21%. In comparison with the first category, small increases in rejection and flux were observed. It can be explained that for the second category, because of the presence of pressure, chitosan could be deposited on both surface and pore

walls of the membranes, resulting in a small increase of water flux due to the presence of -NH₂ and -OH functional groups on the surface and wall of PES membrane [15]. On the other hand, the rejection capability of $T_{1.5-0.05}$ towards copper ions was obtained to be about 84.65%, which was clearly higher than that of other uncross-linked or cross-linked samples. The reason for the changes has already been explained in section 3.2.2.

AFM images of $T_{1.5}$ and $T_{1.5-0.2}$ clearly demonstrated that the membranes in the second category presented lower roughness than the first category (Fig. S9). The values of S_a, S_q, and S_z for $T_{1.5}$ were 5.99, 7.36, and 43.5 nm, which were changed to 16.8, 21.1, and 94.7 nm for $T_{1.5-0.2}$, respectively (Table S4). On the other hand, the mean size of surface valleys of $T_{1.5}$ was about 105 nm which decreased to 73 nm in $T_{1.5-0.2}$. Accordingly, the second category showed relatively smaller size of hole as well as smoother surface in comparison with the first category.

Fig. 7 represents the surface images and cross sectional morphology of the membranes in the second category. As can be clearly seen, the surface morphology of STPP-modified membranes (Fig. 7(b), (c), (d), and (e)) presented rougher surface than $T_{1.5}$ (Fig. 7(a)). Although there were no observable cracks in the structure of the fabricated membranes, lower rejection and higher flux of $T_{1.5-0.5}$ compared to other STPP modified membranes could be explained, as stated previously, through the repulsion of functional groups of STPP at the highest concentration of STPP. We believe that the presence of pressure to introduce CS into the pores of the modified membranes was a significant factor influencing the lower roughness of the second category of membranes compared to those in the first one. Furthermore, the cross section images of CS-modified membrane (Fig. 7(f)) through the second category demonstrated that the thickness of the CS layer was smaller than that of CS-modified membranes fabricated through the first approach.

In addition, the MWCO curves of the membranes of the second category proved the explanation mentioned previously (Fig. 8). Generally, MWCO of the second category membranes was slightly lower than that of the modified membranes in the first one. Accordingly, the MWCOs of $T_{1.5}$, $T_{1.5-0.05}$, $T_{1.5-0.1}$, and $T_{1.5-0.2}$ were obtained to be about 390, 350, 320 and 305 Da, respectively. In this category, $T_{1.5-0.5}$ showed a similar trend with $M_{1.5-0.5}$ at first category. As mentioned, the modification of either surface or pores of the membranes caused higher rejection capability of the second category.

However, in comparison, the rejection ability and strength of some membranes prepared of chitosan has been tabulated in Table S5. As a consequence, none of the prepared membranes in the list showed highest rejection of NaCl in comparison with the membrane modified by our procedure. The highest value of NaCl rejection tabulated in Table S5 is nearly 64%, which is markedly lower than that of modified membranes in this work, which was reported to be about 97%.

CONCLUSION

According to our study, the prepared thin film chitosan nanofiltration membranes were cross-linked by STPP. The effect of STPP concentration on the performance and morphology of TFC nano-
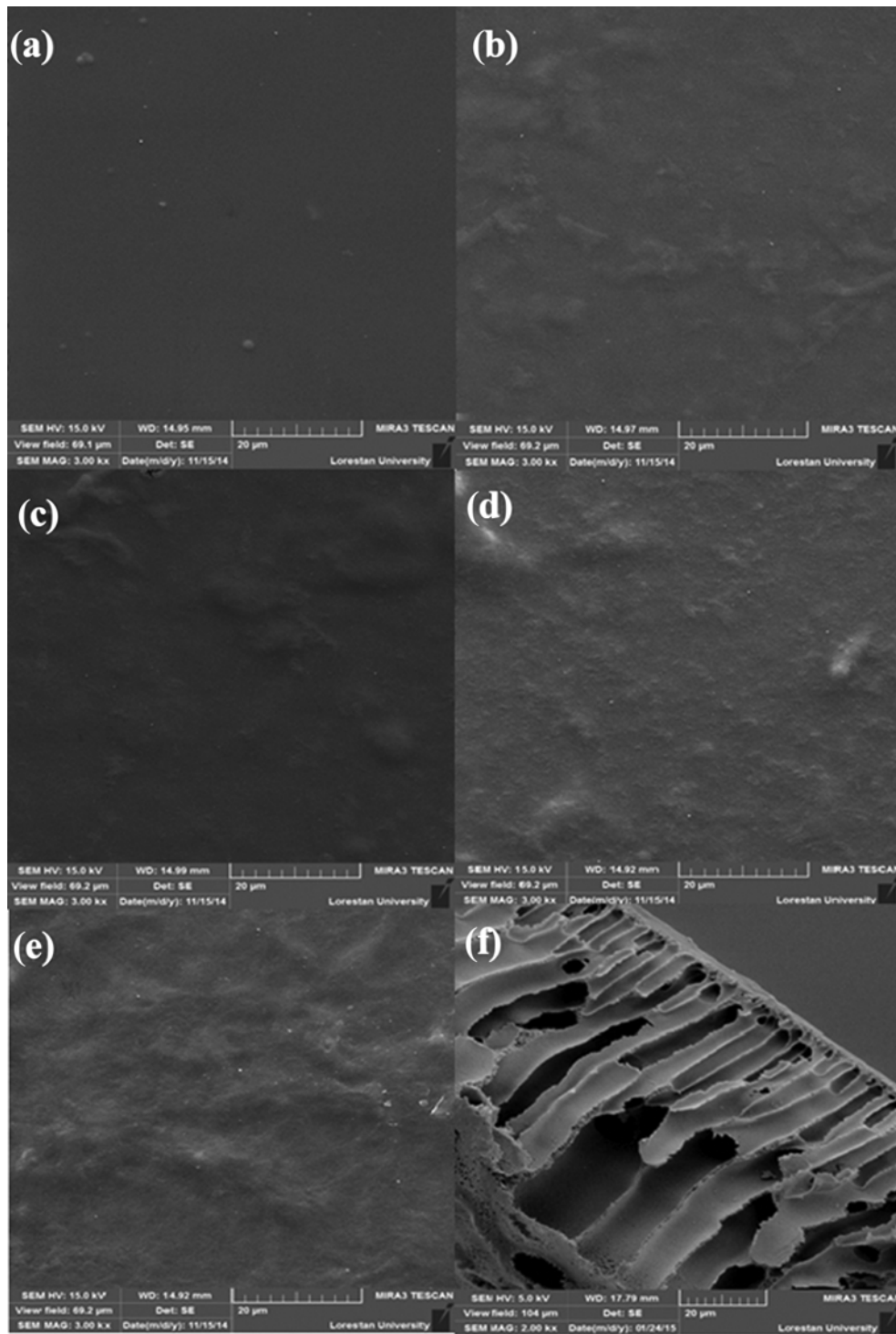
Fig. 7. SEM surface image of: (a) T$_{1.5}$, (b) T$_{1.5\text{-}0.05}$, (c) T$_{1.5\text{-}0.1}$, (d) T$_{1.5\text{-}0.2}$ and (e) T$_{1.5\text{-}0.5}$ and (f) cross-section structure of T$_{1.5}$ membrane.

filtration membranes was investigated. ATR-IR, SEM and AFM analyses showed that thin layers were fabricated on the support layer. Moreover, SEM and AFM images represented that the membrane surfaces became denser and rougher by increasing STPP concentration. Accordingly, the NaCl rejection of CS-modified membranes was increased from 52 to about 97%. The reason for relatively less rejection of CuSO$_4$ solution would be attributed to

the adsorption of copper ions on the surface, due to some characteristics of STPP, such as not only the presence of negatively charged moieties but also slight mitigation of positively charged surface and less availability of -NH$_2$ groups. The surface adsorption characteristics of CS membranes were improved by using STPP. The membranes prepared by second approach revealed increasing hydrophilicity due to the deposition of chitosan on the membrane
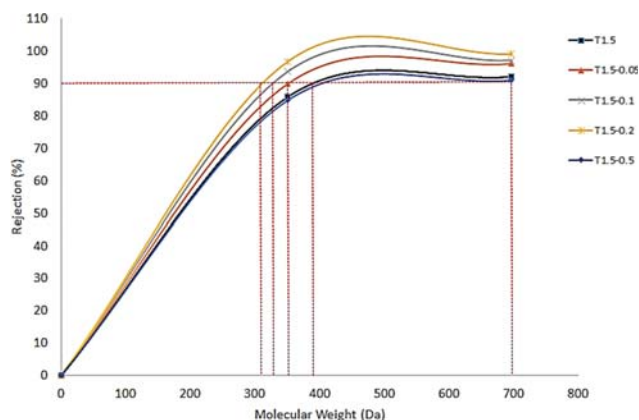
Fig. 8. MWCO graphs of the composite membranes (the second category).

surface as well as pore wall. However, the composite membranes prepared by second method showed high flux and fairly good rejection towards inorganic salts.

ABBREVIATIONS

AA   : acrylic acid
AFM   : atomic force microscopy
ATR-IR   : attenuated total reflectance-infrared spectroscopy
CS   : chitosan
DMF   : N, N-dimethylformamide
NF   : nanofiltration
PEG   : polyethylene glycol
PES   : polyethersulfone
PVP   : polyvinylpyrrolidone
SEM-EDX : scanning electron microscopy-energy dispersive X-ray
              spectroscopy
STPP   : sodium tripolyphosphate

SUPPORTING INFORMATION

Additional information as noted in the text. This information is available via the Internet at http://www.springer.com/chemistry/journal/11814.

REFERENCES

1. Seema S. Shenvi, Suraya A. Rashid, A. F. Ismail, M. A. Kassim and Arun M. Isloor, *Desalination*, **315**, 135 (2013).
2. Y. Mansourpanah and Z. Amiri, *Desalination*, **335**, 33 (2014).
3. E. Bet-Moushoul, Y. Mansourpanah, Kh. Farhadi and A. M. Nik-bakht, *Energy Fuels*, **30**(5), 4085 (2016).
4. J. Miao, L. Zhang and H. Lin, *Chem. Eng. Sci.*, **87**, 152 (2013).
5. Q. Wang, G. Zhang, Zh. Li, Sh. Deng, H. Chen and P. Wang, *Desalination*, **352**, 38 (2014).
6. J. Jin, D. Liu, D. Zhang, Yu. Yin, Xin. Zhao and Yu. Zhang, *Desalination*, **355**, 141 (2015).
7. M. Khayet, *Adv. Colloid Interface Sci.*, **164**(1-2), 56 (2011).
8. Y. Ji, Q. An, F. Zhao and C. Gao, *Desalination*, **357**, 8 (2015).
9. X. Qu, P. J. J. Alvarez and Q. Li, *Water Res.*, **47**, 3931 (2013).
10. F. Ge, M. Li, H. Ye and B. Zhao, *J. Hazard. Mater.*, **211-212**, 366 (2012).
11. R. Kumar, A. M. Isloor and A. F. Ismail, *Desalination*, **350**, 102 (2014).
12. W. P. Zhu, J. Gao, Sh. P. Sun, S. Zhang and T. Sh. Chung, *J. Membr. Sci.*, **487**, 117 (2015).
13. Ch. Zhou, X. l. Gao, S. Li and C. Gao, *Desalination*, **317**, 67 (2013).
14. Y. Osada and T. Nakagawa, *Membrane science and technology*, CRC Press, New York, 289 (1992).
15. S. Boributh, A. Chanachai and R. Jiraratananon, *J. Membr. Sci.*, **342**, 97 (2009).
16. J. Miao, G. Chenc, C. Gaoc and Sh. Dong, *Desalination*, **233**, 147 (2008).
17. D. A. Musale, A. Kumar and G. Pleizier, *J. Membr. Sci.*, **154**, 163 (1999).
18. U. K. Aravind, Ji. Mathew and C. T. Aravindakumar, *J. Membr. Sci.*, **299**, 146 (2007).
19. P. Daraei, S. S. Madaeni, E. Salehi, N. Ghaemi, H. Sadeghi Ghari, M. A. Khadivi and E. Rostami, *J. Membr. Sci.*, **436**, 97 (2013).
20. Y. Ch. Huang and T. J. Liu, *Acta Biomater.*, **8**, 1048 (2012).
21. S. Shenvi, A. F. Ismail and A. M. Isloor, *Desalination*, **344**, 90 (2014).
22. A. Ghaee, M. Shariaty-Niassar, J. Barzin and T. Matsuura, *Chem. Eng. J.*, **165**, 46 (2010).
23. E. Salehi, S. S. Madaeni, L. Rajabi, V. Vatanpour, A. A. Derakhshan, S. Zinadini, Sh. Ghorabi and H. Ahmadi Monfared, *Sep. Purif. Technol.*, **89**, 309 (2012).
24. Y. Mansourpanah, S. S. Madaeni and A. Rahimpour, *Sep. Purif. Technol.*, **69**, 234 (2009).
25. J. Zhu, M. Tian, Y. Zhang, H. Zhang and J. Liu, *Chem. Eng. J.*, **265**, 184 (2015).
26. S. T. Lee, F. L. Mi, Y. J. Shen and Sh. Sh. Shyu, *Polymer*, **42**, 1879 (2001).
27. D. R. Bhumkar and V. B. Pokharkar, *AAPS Pharm. Sci. Tech.*, **7**, E138 (2006).
28. P. Sun, M. Zhu, K. Wang, M. Zhong, J. Wei, D. Wu, Zh. Xu and H. Zhu, *ACS Nano*, **7**, 428 (2013).
29. Y. Mansourpanah, S. S. Madaeni and A. Rahimpour, *J. Membr. Sci.*, **343**, 219 (2009).
30. Y. Luo, B. Zhang, W. H. Cheng and Q. Wang, *Carbohydr. Polym.*, **82**, 942 (2010).
31. M. K. Sureshkumar, D. Das, M. B. Mallia and P. C. Gupta, *J. Hazard. Mater.*, **184**, 65 (2010).
32. B. B. Vyas and P. Ray, *Desalination*, **362**, 104 (2015).
33. T. Mu, Y. Cong, W. Wang and B. Zhang, *Desalination*, **298**, 67 (2012).
34. S. Shenvi, A. F. Ismail and A. M. Isloor, *Desalination*, **344**, 90 (2014).
35. Q. Wang, G. S. Zhang, Z. S. Li, S. Deng, H. Chen and P. Wang, *Desalination*, **352**, 38 (2014).
36. J. Zhu, M. Tian, Y. Zhang, H. Zhang and J. Liu, *Chem. Eng. J.*, **265**, 184 (2015).